

## Lewis-Base Adducts of Group 11 \* Metal(I) Compounds. Part 27.† Solid-state Phosphorus-31 Cross-polarization Magic-angle Spinning Nuclear Magnetic Resonance, Far-infrared, and Structural Studies‡ on the Mononuclear 2:1 Adducts of Triphenylphosphine with Copper(I) and Gold(I) Halides

Graham A. Bowmaker

Department of Chemistry, University of Auckland, Private Bag, Auckland, New Zealand

Jeffrey C. Dyason and Peter C. Healy

School of Science, Griffith University, Nathan, Queensland 4111, Australia

Lutz M. Engelhardt, Chaveng Pakawatchai, and Allan H. White

Department of Physical and Inorganic Chemistry, University of Western Australia, Nedlands 6009, Australia

Single-crystal X-ray diffraction structure determinations, high resolution solid-state cross-polarization magic-angle spinning  $^{31}\text{P}$  n.m.r., and far-i.r. spectral data are reported for the mononuclear 2:1 adducts of triphenylphosphine with copper(I) and gold(I) halides,  $[\text{M}(\text{PPh}_3)_2\text{X}]$ . Crystal data are reported for  $[\text{Cu}(\text{PPh}_3)_2\text{Cl}] \cdot 0.5\text{C}_6\text{H}_6$ ,  $[\text{Cu}(\text{PPh}_3)_2\text{I}]$ ,  $[\text{Au}(\text{PPh}_3)_2\text{Cl}]$  (unsolvated),  $[\text{Au}(\text{PPh}_3)_2\text{Br}]$ , and  $[\text{Au}(\text{PPh}_3)_2\text{I}]$ . In each structure the  $\text{PPh}_3$  ligands adopt an eclipsed conformation about M–P with respect to M–X, with X–M–P–C(11) conformational angles ranging from 0.5 to 18.3°. Within each halide series, M–P distances and P–M–P angles are independent of halogen [CuCl: 2.272(2), 2.260(2) Å, 125.48(7)°; CuI: 2.273(2) Å, 126.9(1)°; AuCl (unsolvated): 2.336(4), 2.317(4) Å, 135.7(1); AuBr: 2.323(2) Å, 132.45(8)°; and AuI: 2.333(2) Å, 132.13(7)°]. Considerable asymmetry (490–560 Hz) in the solid-state  $^{31}\text{P}$  n.m.r. quartets obtained for M = Cu reflects the lower symmetry of the copper environment relative to four-co-ordinate tetrahedral compounds. Solid-state  $^{31}\text{P}$  chemical shift data for M = Au are independent of halogen (Cl, 37; Br, 38; I, 36 p.p.m.). The far-i.r. spectrum of  $[\text{Cu}(\text{PPh}_3)_2\text{I}]$  reveals a strong band at 184  $\text{cm}^{-1}$  which is assigned to the CuI terminal stretching mode.

The 2:1 adducts of unidentate nitrogen and phosphorus bases, L, with univalent coinage metal halides, MX, yield molecular species which are either monomers,  $[\text{ML}_2\text{X}]$ , or di- $\mu$ -halogeno-bridged dimers,  $[\text{L}_2\text{MX}_2\text{ML}_2]$ . Both species are well established with nitrogen bases for  $\text{CuX}$ <sup>1,2</sup> although much less so for  $\text{AgX}$  and  $\text{AuX}$ . Structural studies on compounds with phosphine bases have shown that the triphenylphosphine adduct  $[\text{Cu}(\text{PPh}_3)_2\text{Br}]$  (as its benzene solvate)<sup>3</sup> is monomeric, but that the sulphur dioxide 'solvate' of  $[\text{Cu}(\text{PPh}_2\text{Me})_2\text{I}]$  is dimeric.<sup>4</sup> For triphenylphosphine, dimeric species are formed but in the unique stoichiometric ratio of 1:1.5,  $[(\text{PPh}_3)_2\text{CuX}_2 \cdot \text{Cu}(\text{PPh}_3)]$ .<sup>5</sup> With silver, structure determinations for  $[\text{Ag}(\text{PPh}_3)_2\text{X}]$  have revealed only dimeric species for X = Cl<sup>6</sup> and Br<sup>7</sup> but for gold, the structure of  $[\text{Au}(\text{PPh}_3)_2\text{Cl}]$ , both as its benzene solvate<sup>8</sup> and unsolvated,<sup>9</sup> has been shown to be again monomeric, with the benzene solvate isostructural with the CuBr analogue.

These results are both diverse and sporadic and, given the differences in the chemistry of copper(I) and gold(I), the similarity of the structural results for the CuBr and AuCl adducts seems surprising. It was not obvious to us that all the compounds in the series  $[\text{M}(\text{PPh}_3)_2\text{X}]$  (M = Cu or Au; X = Cl, Br, or I) would be mononuclear; indeed the existence of the CuI adduct as either a monomer or a dimer was not firmly established synthetically. As part of our studies on the structural and spectroscopic properties of the adducts of triphenylphosphine with univalent coinage metal halides we have

synthesized these compounds, completing structural, solid-state  $^{31}\text{P}$  n.m.r., and far-i.r. spectroscopic analysis on the series.

### Experimental

**Preparation of Compounds.**— $[\text{Cu}(\text{PPh}_3)_2\text{Cl}] \cdot 0.5\text{C}_6\text{H}_6$ ,<sup>3</sup>  $[\text{Cu}(\text{PPh}_3)_2\text{Br}] \cdot 0.5\text{C}_6\text{H}_6$ ,<sup>3</sup>  $[\text{Cu}(\text{PPh}_3)_2(\text{NO}_3)]$ ,<sup>10</sup>  $[\text{Cu}(\text{PPh}_3)_2(\text{BH}_4)]$ ,<sup>11</sup>  $[\text{Au}(\text{PPh}_3)_2\text{Cl}] \cdot 0.5\text{C}_6\text{H}_6$ ,<sup>8,12</sup>  $[\text{Au}(\text{PPh}_3)_2\text{Br}]$ ,<sup>12</sup> and  $[\text{Au}(\text{PPh}_3)_2\text{I}]$ <sup>12</sup> were all prepared according to published procedures.

Crystals of the previously unreported  $[\text{Cu}(\text{PPh}_3)_2\text{I}]$  suitable for X-ray crystallography were isolated from the reaction of equimolar quantities of KI and  $[\text{Cu}(\text{PPh}_3)_2(\text{NO}_3)]$  in acetonitrile–chloroform (1:1). Bulk samples of the compound were more conveniently prepared, however, by the direct reaction of stoichiometric quantities of CuI and  $\text{PPh}_3$  in refluxing acetonitrile. Typically, CuI (0.5 g) and  $\text{PPh}_3$  (1.3 g) were refluxed overnight in  $\text{CH}_3\text{CN}$  (100  $\text{cm}^3$ ). Well formed crystals of the compound were obtained by slow cooling of the filtered reaction mixture, m.p. 182 °C (Found: C, 60.9; H, 4.3. Calc. for  $\text{C}_{36}\text{H}_{30}\text{CuI}_2$ : C, 60.5; H, 4.2%). [Note: despite reasonably satisfactory analysis figures, solid-state  $^{31}\text{P}$  n.m.r. spectra nevertheless showed that small amounts of the 1.5:1 dimer were present in each sample prepared.]

Untwinned crystals of unsolvated  $[\text{Au}(\text{PPh}_3)_2\text{Cl}]$ <sup>9</sup> were prepared by the slow evaporation of a stoichiometric quantity of  $\text{PPh}_3$  and  $[\text{Au}(\text{PPh}_3)\text{Cl}]$  dissolved in warm toluene.

**Spectroscopy.**—Solid-state  $^{31}\text{P}$  spectra of the compounds were obtained at room temperature on a Bruker CXP-300 spectrometer at 121.47 MHz using  $^1\text{H}$ – $^{31}\text{P}$  cross polarization with radiofrequency fields of 8 and 20 G ( $G = 10^{-4}\text{T}$ ) respectively as described previously.<sup>13</sup> Chemical shift data were referenced to 85%  $\text{H}_3\text{PO}_4$  via solid triphenylphosphine ( $\delta -9.9$

\* Formerly Group 1B; refers to new 18-Group format of the Periodic Table.

† Part 26 is ref. 19.

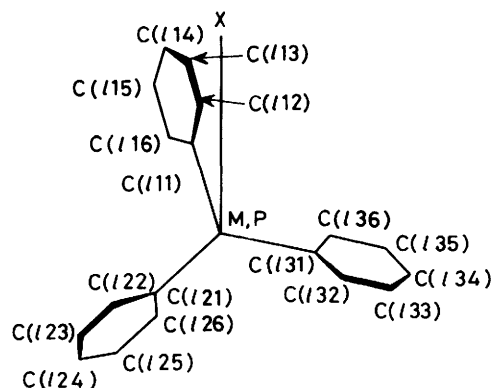
‡ Supplementary data available: see Instructions for Authors, *J. Chem. Soc., Dalton Trans.*, 1987, Issue 1, pp. xvii–xx.

**Table 1.** Non-hydrogen atom co-ordinates for  $[\text{Cu}(\text{PPh}_3)_2\text{Cl}]\cdot 0.5\text{C}_6\text{H}_6$ 

| Atom    | Ligand 1    |             |             | Ligand 2    |             |            |
|---------|-------------|-------------|-------------|-------------|-------------|------------|
|         | x           | y           | z           | x           | y           | z          |
| Cu      | 0.126 37(5) | 0.288 99(6) | 0.255 90(5) |             |             |            |
| Cl      | 0.153 6(1)  | 0.443 2(2)  | 0.179 4(1)  |             |             |            |
| P(l)    | 0.279 2(1)  | 0.186 4(1)  | 0.352 6(1)  | -0.040 0(1) | 0.239 5(1)  | 0.231 2(1) |
| C(l11)  | 0.406 6(4)  | 0.235 6(5)  | 0.355 0(4)  | -0.158 3(4) | 0.346 5(5)  | 0.164 4(4) |
| C(l12)  | 0.405 1(4)  | 0.371 4(5)  | 0.354 6(5)  | -0.142 1(4) | 0.431 3(6)  | 0.105 0(4) |
| C(l13)  | 0.502 5(5)  | 0.413 6(6)  | 0.366 7(5)  | -0.232 1(5) | 0.512 5(6)  | 0.053 3(4) |
| C(l14)  | 0.600 3(4)  | 0.319 1(6)  | 0.376 9(4)  | -0.335 8(4) | 0.509 2(6)  | 0.062 2(4) |
| C(l15)  | 0.602 9(4)  | 0.183 3(6)  | 0.373 8(4)  | -0.351 7(4) | 0.427 4(6)  | 0.121 8(4) |
| C(l16)  | 0.506 0(4)  | 0.140 9(5)  | 0.363 1(4)  | -0.263 4(4) | 0.344 8(5)  | 0.172 7(4) |
| C(l21)  | 0.311 6(4)  | -0.001 5(5) | 0.303 0(4)  | -0.083 8(3) | 0.259 6(5)  | 0.355 9(4) |
| C(l22)  | 0.320 7(5)  | -0.048 9(6) | 0.198 3(4)  | -0.098 5(4) | 0.393 8(5)  | 0.419 1(4) |
| C(l23)  | 0.338 9(5)  | -0.190 5(6) | 0.155 2(4)  | -0.120 5(4) | 0.416 8(5)  | 0.517 5(4) |
| C(l24)  | 0.343 3(5)  | -0.285 1(6) | 0.215 3(5)  | -0.129 4(4) | 0.307 2(6)  | 0.557 0(4) |
| C(l25)  | 0.333 6(4)  | -0.239 4(5) | 0.317 1(4)  | -0.116 8(4) | 0.174 2(6)  | 0.495 8(4) |
| C(l26)  | 0.318 3(4)  | -0.098 5(5) | 0.361 9(4)  | -0.095 0(4) | 0.150 9(5)  | 0.395 4(4) |
| C(l31)  | 0.275 0(4)  | 0.206 3(5)  | 0.490 9(4)  | -0.043 3(4) | 0.060 0(5)  | 0.165 2(4) |
| C(l32)  | 0.179 2(4)  | 0.200 5(6)  | 0.518 5(4)  | 0.034 3(4)  | -0.046 6(5) | 0.203 4(4) |
| C(l33)  | 0.171 2(4)  | 0.213 3(6)  | 0.621 9(5)  | 0.035 1(5)  | -0.185 5(5) | 0.157 4(4) |
| C(l34)  | 0.257 4(5)  | 0.233 1(6)  | 0.697 8(4)  | -0.040 0(5) | -0.218 1(5) | 0.072 9(5) |
| C(l35)  | 0.354 0(5)  | 0.240 8(7)  | 0.671 0(4)  | -0.113 7(5) | -0.114 3(6) | 0.031 5(5) |
| C(l36)  | 0.361 5(4)  | 0.226 6(6)  | 0.568 5(4)  | -0.116 6(4) | 0.024 1(6)  | 0.077 7(4) |
| Solvent |             |             |             |             |             |            |
| C(1)    | 0.414 1(6)  | 0.110 4(8)  | -0.000 3(7) |             |             |            |
| C(2)    | 0.499 7(7)  | 0.110 4(8)  | 0.080 1(6)  |             |             |            |
| C(3)    | 0.416 8(7)  | -0.001 1(9) | -0.078 3(6) |             |             |            |

**Table 2.** Non-hydrogen atom co-ordinates for  $[\text{Cu}(\text{PPh}_3)_2\text{I}]$ 

| Atom  | x           | y            | z             |
|-------|-------------|--------------|---------------|
| Cu    | 0           | 0.108 3(1)   | $\frac{1}{4}$ |
| I     | 0           | 0.385 91(8)  | $\frac{1}{4}$ |
| P     | 0.090 19(7) | -0.003 6(2)  | 0.294 1(1)    |
| C(11) | 0.155 6(3)  | 0.114 1(7)   | 0.317 0(4)    |
| C(12) | 0.158 2(3)  | 0.250 1(9)   | 0.358 6(5)    |
| C(13) | 0.208 0(4)  | 0.340 3(9)   | 0.381 6(7)    |
| C(14) | 0.253 9(4)  | 0.294 7(10)  | 0.362 5(6)    |
| C(15) | 0.251 8(4)  | 0.160 7(11)  | 0.320 8(6)    |
| C(16) | 0.201 8(3)  | 0.067 6(8)   | 0.297 1(5)    |
| C(21) | 0.088 0(3)  | -0.130 1(7)  | 0.201 0(5)    |
| C(22) | 0.074 8(3)  | -0.071 1(8)  | 0.109 9(5)    |
| C(23) | 0.067 8(4)  | -0.163 1(9)  | 0.033 5(6)    |
| C(24) | 0.073 2(4)  | -0.311 8(10) | 0.048 0(6)    |
| C(25) | 0.085 6(3)  | -0.371 0(8)  | 0.136 2(6)    |
| C(26) | 0.093 3(3)  | -0.281 5(7)  | 0.213 0(5)    |
| C(31) | 0.116 4(3)  | -0.117 1(7)  | 0.403 1(4)    |
| C(32) | 0.074 4(3)  | -0.197 8(7)  | 0.418 4(5)    |
| C(33) | 0.092 0(3)  | -0.286 9(8)  | 0.499 4(6)    |
| C(34) | 0.150 4(4)  | -0.289 6(8)  | 0.566 7(5)    |
| C(35) | 0.192 9(3)  | -0.208 3(9)  | 0.552 3(6)    |
| C(36) | 0.176 1(3)  | -0.122 9(8)  | 0.470 9(5)    |



**Structure Determinations.**—Unique data sets were measured to the specified  $2\theta_{\text{max}}$  limits on specimens mounted in capillaries using Syntex  $PT$  and Enraf-Nonius CAD-4 four-circle diffractometers (monochromatic  $\text{Mo-K}\alpha$  radiation sources,  $\lambda = 0.71069$  Å) in conventional  $2\theta$ - $\theta$  scan mode, at 295 K.  $N$  Independent reflections were measured,  $N_o$  with  $I > 3\sigma(I)$  being considered 'observed' and used in the large block least-squares refinement with statistical weights after solution of the structures by the heavy-atom method. Data were corrected for absorption (analytical correction);  $(x, y, z, U_{\text{iso}})_{\text{H}}$  were included at idealized values. Residuals on  $|F|$  at convergence were  $R, R'$ . Neutral complex scattering factors were used.<sup>14</sup> Computation used the XTAL83 program system<sup>15</sup> implemented by S. R. Hall on a Perkin-Elmer 3240 computer, and the APPLECRYST program package, written by C. H. L. Kennard for an APPLE IIe microcomputer. Non-hydrogen atom co-ordinates are given in Tables 1–4. The atom labelling scheme adopted for the  $\text{PPh}_3$  ligands is shown above. The carbon atoms  $C(lm2)$  ( $m = \text{ring}$

p.p.m.). Far-i.r. spectra were recorded at ca. 298 and ca. 125 K as petroleum jelly mulls between Polythene plates on a Grubb-Parsons MkII cube interferometer interfaced to a CBM PET microcomputer, and were calibrated against the spectrum of water vapour.

**Table 3.** Non-hydrogen atom co-ordinates for  $[\text{Au}(\text{PPh}_3)_2\text{Cl}]$ 

| Atom            | Ligand 1    |             |              | Ligand 2    |              |              |
|-----------------|-------------|-------------|--------------|-------------|--------------|--------------|
|                 | x           | y           | z            | x           | y            | z            |
| Cl              | 0.095 2(3)  | 0.236 8(3)  | 0.432 6(3)   |             |              |              |
| Au              | 0.225 69(4) | 0.259 64(5) | 0.286 91(4)  |             |              |              |
| P( <i>l</i> )   | 0.223 4(2)  | 0.406 7(3)  | 0.188 9(3)   | 0.301 8(2)  | 0.117 4(3)   | 0.263 8(3)   |
| C( <i>l</i> 11) | 0.145 5(8)  | 0.496 1(10) | 0.243 4(10)  | 0.296 7(8)  | 0.040 7(10)  | 0.384 3(11)  |
| C( <i>l</i> 12) | 0.127 3(8)  | 0.522 0(10) | 0.369 3(10)  | 0.216 0(9)  | 0.026 1(12)  | 0.456 7(11)  |
| C( <i>l</i> 13) | 0.071 0(10) | 0.591 8(11) | 0.409 6(11)  | 0.206 6(10) | -0.038 2(13) | 0.542 2(13)  |
| C( <i>l</i> 14) | 0.032 3(10) | 0.636 1(12) | 0.327 7(13)  | 0.272 1(11) | -0.090 4(13) | 0.559 8(13)  |
| C( <i>l</i> 15) | 0.050 6(10) | 0.610 6(12) | 0.201 4(13)  | 0.350 8(11) | -0.080 2(13) | 0.490 1(14)  |
| C( <i>l</i> 16) | 0.106 3(9)  | 0.541 4(11) | 0.158 0(11)  | 0.362 4(10) | -0.017 1(13) | 0.399 7(13)  |
| C( <i>l</i> 21) | 0.167 6(8)  | 0.312 1(10) | 0.010 5(10)  | 0.441 8(9)  | 0.200 7(11)  | 0.273 4(12)  |
| C( <i>l</i> 22) | 0.073 8(9)  | 0.192 2(12) | -0.030 2(12) | 0.507 2(11) | 0.317 1(14)  | 0.387 9(14)  |
| C( <i>l</i> 23) | 0.030 4(10) | 0.113 2(12) | -0.166 8(13) | 0.612 6(12) | 0.387 1(16)  | 0.393 4(19)  |
| C( <i>l</i> 24) | 0.077 2(10) | 0.153 8(13) | -0.261 8(12) | 0.656 5(12) | 0.347 6(21)  | 0.293 3(21)  |
| C( <i>l</i> 25) | 0.166 4(11) | 0.269 7(15) | -0.220 2(12) | 0.590 8(14) | 0.234 5(22)  | 0.180 8(20)  |
| C( <i>l</i> 26) | 0.213 6(9)  | 0.351 2(12) | -0.085 0(11) | 0.487 9(11) | 0.164 4(17)  | 0.173 5(16)  |
| C( <i>l</i> 31) | 0.356 3(9)  | 0.533 7(11) | 0.205 1(11)  | 0.244 0(8)  | -0.018 3(10) | 0.100 1(11)  |
| C( <i>l</i> 32) | 0.437 7(11) | 0.500 3(15) | 0.203 1(17)  | 0.214 5(12) | 0.007 8(13)  | -0.007 6(13) |
| C( <i>l</i> 33) | 0.536 2(12) | 0.586 5(19) | 0.206 0(21)  | 0.163 8(13) | -0.091 5(16) | -0.132 5(13) |
| C( <i>l</i> 34) | 0.558 1(12) | 0.712 7(16) | 0.213 6(18)  | 0.143 0(11) | -0.220 7(15) | -0.155 9(13) |
| C( <i>l</i> 35) | 0.479 1(13) | 0.747 0(14) | 0.212 3(20)  | 0.173 9(12) | -0.249 7(13) | -0.053 1(15) |
| C( <i>l</i> 36) | 0.380 4(11) | 0.660 3(12) | 0.209 0(17)  | 0.224 3(10) | -0.147 1(12) | 0.075 7(12)  |

**Table 4.** Non-hydrogen atom co-ordinates for  $[\text{Au}(\text{PPh}_3)_2\text{X}]$  (X = Br or I)

| Atom  | X = Br      |              |               | X = I       |              |               |
|-------|-------------|--------------|---------------|-------------|--------------|---------------|
|       | x           | y            | z             | x           | y            | z             |
| Au    | 0           | 0.096 78(6)  | $\frac{1}{4}$ | 0           | 0.097 50(4)  | $\frac{1}{4}$ |
| X     | 0           | 0.386 9(2)   | $\frac{1}{4}$ | 0           | 0.399 00(9)  | $\frac{1}{4}$ |
| P     | 0.093 91(8) | -0.006 7(2)  | 0.294 2(1)    | 0.093 98(8) | -0.006 1(2)  | 0.294 9(1)    |
| C(11) | 0.157 0(3)  | 0.114 5(9)   | 0.317 5(5)    | 0.157 1(3)  | 0.111 6(8)   | 0.318 5(5)    |
| C(12) | 0.155 9(3)  | 0.258 9(10)  | 0.348 5(6)    | 0.158 7(4)  | 0.249 8(10)  | 0.354 5(8)    |
| C(13) | 0.204 9(4)  | 0.351 4(11)  | 0.372 7(7)    | 0.207 2(5)  | 0.342 1(12)  | 0.375 5(9)    |
| C(14) | 0.254 3(4)  | 0.301 1(12)  | 0.363 3(7)    | 0.254 5(5)  | 0.295 0(14)  | 0.363 8(8)    |
| C(15) | 0.255 5(4)  | 0.162 2(12)  | 0.330 7(7)    | 0.254 0(4)  | 0.159 1(15)  | 0.326 9(8)    |
| C(16) | 0.206 9(4)  | 0.064 9(10)  | 0.306 4(6)    | 0.205 3(4)  | 0.065 3(11)  | 0.303 6(7)    |
| C(21) | 0.089 8(3)  | -0.136 5(9)  | 0.200 9(5)    | 0.090 1(3)  | -0.131 7(8)  | 0.200 5(6)    |
| C(22) | 0.078 2(4)  | -0.076 6(11) | 0.108 9(6)    | 0.076 7(4)  | -0.073 4(10) | 0.109 1(7)    |
| C(23) | 0.068 7(4)  | -0.173 5(12) | 0.030 4(6)    | 0.067 9(5)  | -0.164 7(12) | 0.033 1(7)    |
| C(24) | 0.068 6(4)  | -0.323 9(12) | 0.042 0(7)    | 0.072 4(5)  | -0.314 9(13) | 0.046 3(7)    |
| C(25) | 0.080 2(4)  | -0.380 9(11) | 0.134 7(7)    | 0.085 0(5)  | -0.371 6(10) | 0.134 6(8)    |
| C(26) | 0.090 2(4)  | -0.287 5(9)  | 0.212 7(6)    | 0.094 6(4)  | -0.283 0(9)  | 0.213 8(7)    |
| C(31) | 0.119 8(3)  | -0.117 3(9)  | 0.405 7(5)    | 0.118 6(3)  | -0.118 4(7)  | 0.404 8(5)    |
| C(32) | 0.077 2(3)  | -0.197 3(10) | 0.420 7(6)    | 0.076 6(4)  | -0.198 2(11) | 0.419 1(6)    |
| C(33) | 0.094 8(4)  | -0.284 0(11) | 0.505 3(6)    | 0.093 7(5)  | -0.280 9(11) | 0.502 3(8)    |
| C(34) | 0.153 7(4)  | -0.288 9(10) | 0.574 9(6)    | 0.152 1(5)  | -0.287 3(11) | 0.571 0(7)    |
| C(35) | 0.196 5(4)  | -0.210 4(11) | 0.561 1(6)    | 0.194 9(4)  | -0.209 5(13) | 0.557 9(7)    |
| C(36) | 0.179 8(3)  | -0.124 9(11) | 0.476 6(6)    | 0.178 3(4)  | -0.126 6(10) | 0.474 5(6)    |

number 1, 2, or 3; *l* = ligand number 1 or 2) are defined as those atoms on the same side of the C(*l*11)–C(*l*21)–C(*l*31) plane as the co-ordinated metal atom. Ring 1 is defined as that ring with the lowest conformational angle X–M–P(*l*)–C(*l*m1). Pertinent geometric parameters are given in Tables 5–7. Where structural data have been taken or calculated from published work, the atom labelling has been adjusted to conform with the present system.

*Crystal data.*  $[\text{Cu}(\text{PPh}_3)_2\text{Cl}] \cdot 0.5\text{C}_6\text{H}_6$ .  $\text{C}_{39}\text{H}_{33}\text{ClCuP}_2$ ,  $M = 662.6$ , triclinic, space group  $P\bar{1}$  ( $C_2^1$ , no. 2),  $a = 12.848(5)$ ,  $b = 10.136(5)$ ,  $c = 13.468(5)$  Å,  $\alpha = 104.51(4)$ ,  $\beta = 102.20(3)$ ,  $\gamma = 74.80(4)^\circ$ ,  $U = 1.619(2)$  Å<sup>3</sup>,  $D_m = 1.37(2)$ ,  $D_c$  ( $Z = 2$ ) = 1.36 g cm<sup>-3</sup>,  $F(000) = 686$ ,  $\mu_{\text{Mo}}$  = 7.4 cm<sup>-1</sup>. Specimen: 0.30 × 0.14 × 0.12 mm;  $2\theta_{\text{max}}$  = 50°;  $N = 5715$ ,  $N_o = 3300$ ;  $R = 0.045$ ,  $R' = 0.046$ .

$[\text{Cu}(\text{PPh}_3)_2\text{I}] \cdot \text{C}_3\text{H}_3\text{O}$ ,  $M = 715.1$ , monoclinic, space

**Table 5.** Conformational angles ( $^{\circ}$ ) for  $[M(PPh_3)_2X]$ 

| Compound                                 | <i>l</i> | X-M-P( <i>l</i> )-C( <i>lm1</i> ) |              |              | M-P( <i>l</i> )-C( <i>lm1</i> )-C( <i>lm2</i> ) |              |              |
|--|----------|-----------------------------------|--------------|--------------|---|--------------|--------------|
|  |          | <i>m</i> = 1                      | <i>m</i> = 2 | <i>m</i> = 3 | <i>m</i> = 1                                    | <i>m</i> = 2 | <i>m</i> = 3 |
| $[Cu(PPh_3)_2Cl] \cdot 0.5C_6H_6^a$      | 1        | 1.7                               | 119.0        | -121.3       | -36.8   | -53.4        | -38.5        |
|  | 2        | 9.7                               | 126.9        | -115.6       | -17.5   | -62.9        | -50.7        |
| $[Cu(PPh_3)_2Br] \cdot 0.5C_6H_6^a$      | 1        | -0.5                              | 116.5        | -124.3       | -38.8   | -52.6        | -38.7        |
|  | 2        | 12.9                              | 129.6        | -113.1       | -18.8   | -63.3        | -50.3        |
| $[Cu(PPh_3)_2I]^a$                       | 1        | 4.9                               | 124.0        | -117.5       | -35.2   | -61.1        | -37.4        |
| $[Au(PPh_3)_2Cl]^a$                      | 1        | -7.1                              | 111.9        | -132.2       | -26.8   | -47.6        | -33.1        |
|  | 2        | 18.3                              | 138.1        | -104.8       | -23.4   | -56.4        | -34.8        |
| $[Au(PPh_3)_2Cl] \cdot 0.5C_6H_6^c$      | 1        | 1.7                               | 121.9        | -122.0       | -35.6   | -62.1        | -32.9        |
|  | 2        | 9.1                               | 126.9        | -117.0       | -19.9   | -66.0        | -44.4        |
| $[Au(PPh_3)_2Br]^a$                      | 1        | 3.5                               | 126.2        | -118.2       | -26.2   | -67.8        | -35.6        |
| $[Au(PPh_3)_2I]^a$                       | 1        | 3.6                               | 124.9        | -119.0       | -30.3   | -64.6        | -35.7        |
| $[Cu(PPh_3)_2(BH_4)]^d$                  | 1        | 7.7                               | 125.3        | -115.1       | -35.6   | -61.4        | -37.4        |
| $[Cu(PPh_3)_2(BH_4)] \cdot 0.5C_5H_5N^e$ | 1        | 2.9                               | 117.5        | -121.7       | -43.1   | -51.0        | -39.4        |
|  | 2        | 12.0                              | 127.8        | -113.6       | -21.8   | -59.4        | -48.4        |
| $[Cu(PPh_3)_2(NO_3)]^f$                  | 1        | 7.3                               | 125.4        | -117.0       | -33.3   | -62.8        | -30.6        |

<sup>a</sup> This work. <sup>b</sup> Ref. 3. <sup>c</sup> Ref. 8. <sup>d</sup> Ref. 16. <sup>e</sup> Ref. 17. <sup>f</sup> Ref. 18.

**Table 6.**  $[M(PPh_3)_2X]$  core geometries; distances in Å, angles in  $^{\circ}$ 

| Compound                               | M-P      | M-X      | P-M-P     | P-M-X     | X...H(12) |
|--|----------|----------|-----------|-----------|-----------|
| $[Cu(PPh_3)_2Cl] \cdot 0.5C_6H_6$      | 2.272(2) | 2.208(2) | 125.48(7) | 113.76(7) | 2.89(-)   |
|  | 2.260(2) |          |           | 120.74(6) | 2.83(-)   |
| $[Cu(PPh_3)_2Br] \cdot 0.5C_6H_6^a$    | 2.282(3) | 2.346(2) | 126.0(1)  | 112.8(1)  | 3.01(-)   |
|  | 2.263(2) |          |           | 121.0(1)  | 2.97(-)   |
| $[Cu(PPh_3)_2I]$                       | 2.273(2) | 2.524(2) | 126.9(1)  | 116.61(5) | 2.99(-)   |
| $[Au(PPh_3)_2Cl] \cdot 0.5C_6H_6^b$    | 2.339(4) | 2.500(4) | 132.1(1)  | 109.2(1)  | 2.82(-)   |
|  | 2.323(4) |          |           | 118.7(1)  | 2.89(-)   |
| $[Au(PPh_3)_2Cl]^c$                    | 2.336(4) | 2.533(4) | 135.7(1)  | 109.1(1)  | 2.80(-)   |
|  | 2.317(4) |          |           | 114.8(1)  | 2.69(-)   |
| $[Au(PPh_3)_2Br]$                      | 2.323(2) | 2.625(2) | 132.45(8) | 113.78(5) | 2.82(-)   |
| $[Au(PPh_3)_2I]^d$                     | 2.333(2) | 2.754(1) | 132.13(7) | 113.93(5) | 2.99(-)   |
| $[Cu(PPh_3)_2(BH_4)]$                  | 2.276(2) |          | 123.26(6) |           |           |
| $[Cu(PPh_3)_2(BH_4)] \cdot 0.5C_5H_5N$ | 2.282(2) |          | 123.02(9) |           |           |
|  | 2.271(2) |          |           |           |           |
| $[Cu(PPh_3)_2(NO_3)]$                  | 2.256(3) |          | 131.2(1)  |           |           |

<sup>a</sup> Ref. 3. <sup>b</sup> Ref. 8. <sup>c</sup> Structural data from ref. 9 gives Au-P(1), P(2) = 2.330(9), 2.313(8); Au-Cl = 2.526(10) Å; P-Au-P = 136.4(3); and P-Au-Cl(1), Cl(2) = 108.1(3), 136.4(3) $^{\circ}$ . <sup>d</sup> Au-P = 2.340, Au-I = 2.766 Å, P-Au-P = 131.2, and P-Au-Cl = 114.4 $^{\circ}$ . (J. Strähle and G. Beindorf, personal communication; cited in P. G. Jones, *Gold Bull.*, 1981, 14, 102).

**Table 7.** M-X and M-P distances (Å) in  $[M(PPh_3)_nX]$  compounds (M = Cu or Au; X = Cl, Br, or I); where there is more than one distance, average values are quoted

| Compound         | M-X  |      |      | M-P  |      |      |
|------------------|------|------|------|------|------|------|
|                  | Cl   | Br   | I    | Cl   | Br   | I    |
| $[Au(PPh_3)_3X]$ | 2.28 | 2.41 | 2.55 | 2.23 | 2.25 | 2.25 |
| $[Au(PPh_3)_2X]$ | 2.52 | 2.62 | 2.75 | 2.33 | 2.32 | 2.33 |
| $[Au(PPh_3)_3X]$ | 2.71 |      |      | 2.41 |      |      |
| $[Cu(PPh_3)_2X]$ | 2.21 | 2.35 | 2.52 | 2.26 | 2.27 | 2.27 |
| $[Cu(PPh_3)_3X]$ | 2.34 | 2.48 | 2.67 | 2.35 | 2.35 | 2.36 |

group  $C2/c$  ( $C_{2h}^2$ , no. 15),  $a = 24.90(1)$ ,  $b = 9.094(2)$ ,  $c = 15.493(6)$  Å,  $\beta = 116.74(4)^{\circ}$ ,  $U = 3.133(2)$  Å<sup>3</sup>,  $D_m = 1.54(2)$ ,  $D_c(Z = 4) = 1.52$  g cm<sup>-3</sup>,  $F(000) = 1432$ ,  $\mu_{Mo} = 17.7$  cm<sup>-1</sup>. Specimen: 0.15 × 0.50 × 0.05 mm;  $2\theta_{max} = 50^{\circ}$ ;  $N = 2723$ ,  $N_o = 1587$ ;  $R = 0.039$ ,  $R' = 0.037$ .

$[Au(PPh_3)_2Cl]$ .  $C_{36}H_{30}AuClP_2$ ,  $M = 757.2$ , triclinic, space group  $P1$ ,  $a = 14.317(4)$ ,  $b = 11.866(3)$ ,  $c = 10.911(3)$  Å,  $\alpha = 109.18(2)$ ,  $\beta = 94.38(2)$ ,  $\gamma = 114.10(2)^{\circ}$ ,  $U = 1.550(1)$  Å<sup>3</sup>,  $D_m = 1.63(1)$ ,  $D_c(Z = 2) = 1.62$  g cm<sup>-3</sup>,  $F(000) = 744$ ,  $\mu_{Mo} = 51$  cm<sup>-1</sup>. Specimen: 0.36 × 0.20 × 0.04 mm;  $2\theta_{max} = 50^{\circ}$ ;  $N = 5244$ ,  $N_o = 4405$ ;  $R = 0.049$ ,  $R' = 0.055$ .

$[Au(PPh_3)_2Br]$ .  $C_{36}H_{30}AuBrP_2$ ,  $M = 801.5$ , monoclinic, space group  $C2/c$ ,  $a = 25.051(5)$ ,  $b = 9.048(1)$ ,  $c = 15.292(2)$  Å,  $\beta = 117.58(4)^{\circ}$ ,  $U = 3.072(1)$  Å<sup>3</sup>,  $D_m = 1.72(2)$ ,  $D_c(Z = 4) = 1.73$  g cm<sup>-3</sup>,  $F(000) = 1560$ ,  $\mu_{Mo} = 64$  cm<sup>-1</sup>. Specimen: 0.05 × 0.03 × 0.25 mm;  $2\theta_{max} = 55^{\circ}$ ;  $N = 3519$ ,  $N_o = 2785$ ;  $R = 0.040$ ,  $R' = 0.036$ .

$[Au(PPh_3)_2I]$ .  $C_{36}H_{30}AuIP_2$ ,  $M = 848.5$ , monoclinic, space group  $C2/c$ ,  $a = 25.099(10)$ ,  $b = 9.134(1)$ ,  $c = 15.407(2)$  Å,  $\beta = 117.31(2)^{\circ}$ ,  $U = 3.138(1)$  Å<sup>3</sup>,  $D_m = 1.78(2)$ ,  $D_c(Z = 4) = 1.80$  g cm<sup>-3</sup>,  $F(000) = 1632$ ,  $\mu_{Mo} = 60$  cm<sup>-1</sup>. Specimen: 0.08 × 0.08 × 0.25 mm;  $2\theta_{max} = 65^{\circ}$ ;  $N = 5472$ ,  $N_o = 4165$ ;  $R = 0.058$ ,  $R' = 0.066$ .

The structure of  $[Cu(PPh_3)_2Cl] \cdot 0.5C_6H_6$  was refined in the setting of the isomorphous bromide hemibenzene solvate,<sup>3</sup> and the structures of  $[Cu(PPh_3)_2I]$  and  $[Au(PPh_3)_2X]$  (X = Br or I) refined in the setting of the unsolvated tetrahydroborate.<sup>16</sup>

## Results and Discussion

**Structure Determination.**—Structure determination for each of the complexes studied confirms that the stoichiometric and connectivity properties are as expected for mononuclear halogenobis(triphenylphosphine)metal(I) species. The structure of the CuCl compound is isomorphous with the CuBr

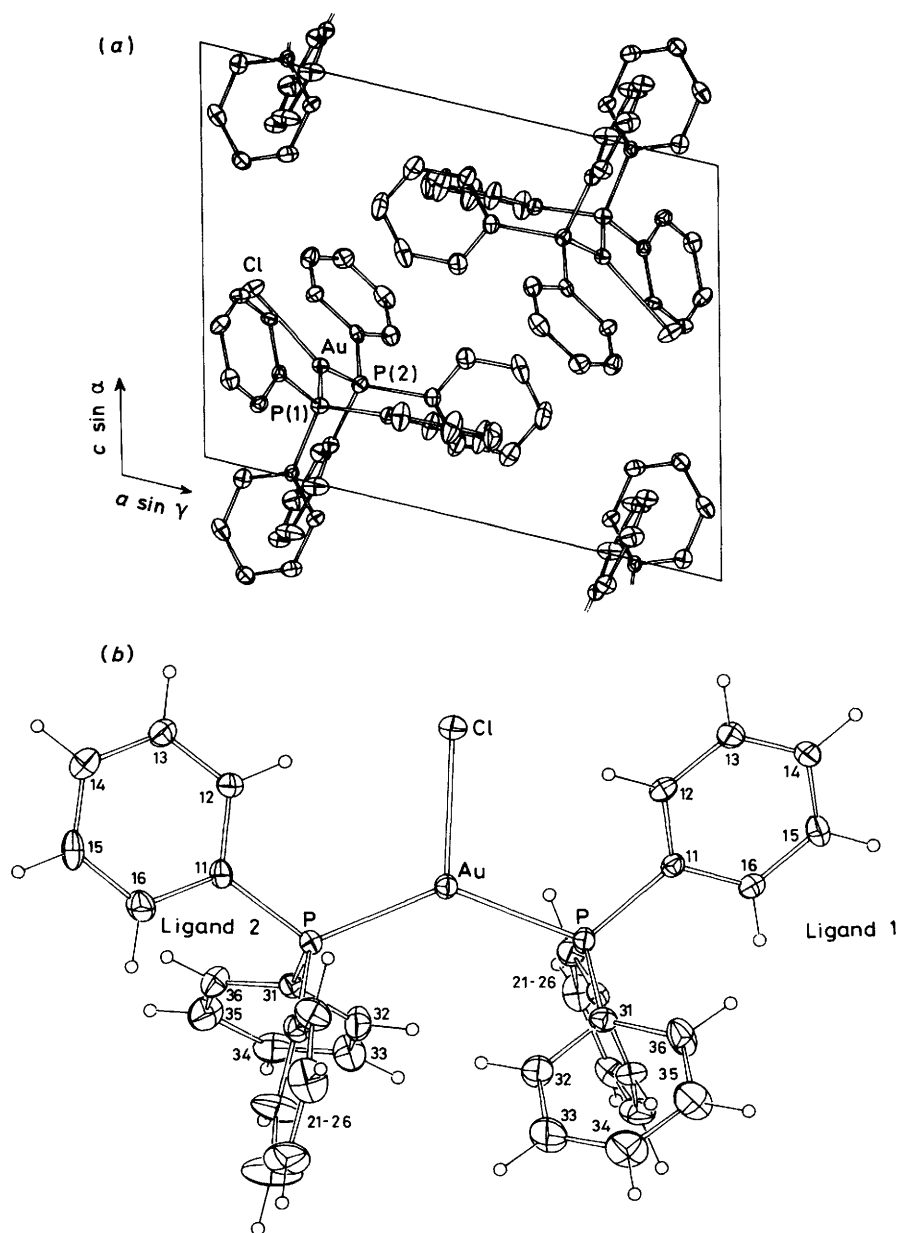


**Figure 1.** (a) The unit-cell contents of unsolvated  $[\text{Au}(\text{PPh}_3)_2\text{Cl}]$  projected down  $b$ . (b) A projection of  $[\text{Au}(\text{PPh}_3)_2\text{Cl}]$  onto the  $\text{P}_2\text{AuCl}$  plane. Hydrogen atoms have an arbitrary radius of 0.1 Å. 20% Thermal ellipsoids are shown in both (a) and (b)

analogue,<sup>3</sup> crystallizing as a hemibenzene solvate. This triclinic structural form is both flexible and accommodating since other isomorphous structures include  $[\text{Cu}(\text{PPh}_3)_2(\text{BH}_4)] \cdot 0.5\text{C}_5\text{H}_5\text{N}$ <sup>17</sup> and  $[\text{Au}(\text{PPh}_3)_2\text{Cl}] \cdot 0.5\text{C}_6\text{H}_6$ <sup>8</sup> (presented in a different setting). The CuI, AuBr, and AuI compounds are also isomorphous with each other and with  $[\text{Cu}(\text{PPh}_3)_2(\text{NO}_3)]$ <sup>18</sup> (presented in a different setting) and  $[\text{Cu}(\text{PPh}_3)_2(\text{BH}_4)]$  (unsolvated).<sup>16</sup> The molecular symmetry in this array is higher than that found in the triclinic lattice above, with the molecule disposed on a crystallographic two-fold symmetry axis coincident with the metal-halogen bond and with one half the molecule comprising the asymmetric unit. The triclinic lattice found for the unsolvated AuCl compound differs from that found for the benzene solvated structure. The structure of this complex has been briefly described previously but only partially refined, data being measured on a twinned crystal.<sup>9</sup> Figure 1(a) and (b) show a cell diagram of  $[\text{Au}(\text{PPh}_3)_2\text{Cl}]$  projected

down the  $b$  axis, and a view of the molecule perpendicular to the  $\text{P}_2\text{AuCl}$  plane.

**Conformational Effects.**—In each structure, the  $\text{PPh}_3$  ligands both adopt eclipsed conformations with  $\text{X-M-P}(l)\text{-C}(l1)$  conformational angles ranging from 0.5 to 18.3° [Figure 1(b)]. For the  $C2/c$  phases, the range and magnitude of this conformational angle is small (3.5–4.9°); by comparison, in the triclinic phases, the ranges for ligands 1 and 2 are 0.5–7.1 and 9.1–18.3° respectively (Table 5). Each ligand approximates to a three-bladed chiral propeller with the pitch of the phenyl rings about P–C, defined here by the angle  $\text{M-P}(l)\text{-C}(l1)\text{-C}(l2)$ , in the ranges 18.8–38.8, 47.6–67.8, and 33.1–50.7° for rings 1, 2, and 3 respectively. These values are comparable to those found for sterically unhindered molecules such as  $[\text{Au}(\text{PPh}_3)\text{X}]$  (average values for  $\text{X} = \text{Cl}, \text{Br}, \text{or I}$ : 33, 55, and 44°),<sup>19</sup> but contrast with those found for  $[\text{Cu}(\text{PPh}_3)_3\text{X}]$ <sup>20</sup> where the pitch

of ring 1 opposes that of each of the other two rings. In both triclinic phases, the magnitude of the X-M-P(*l*)-C(*l*11) angle correlates inversely with the pitch angle of ring 1. The contact distances between the halogen and the *ortho* phenyl hydrogens, H(*l*12), are relatively constant, lying in the range 2.7–3.0 Å (Table 6). A consequence of the W conformational structure adopted by these molecules is that rings 2 and 3 extend above and below the P<sub>2</sub>MX plane providing 'protection' for the metal and halogen atoms (Figure 1).

**Molecular Geometries.**—The P<sub>2</sub>MX core geometries are detailed in Table 6, together with comparative data for [Cu(PPh<sub>3</sub>)<sub>2</sub>(BH<sub>4</sub>)] and [Cu(PPh<sub>3</sub>)<sub>2</sub>(NO<sub>3</sub>)]. The asymmetry observed in the conformational angles for molecules in the triclinic phases is also reflected in differences of 5–9° in the X-M-P angles and a small but consistent difference of the order of 0.01–0.02 Å in the M-P distances. It is of interest to note that, at present, the lower symmetry triclinic phases are found only for the smaller and more electronegative halogens: Cl and Br in the copper compounds, Cl in the gold compounds. Both *P* $\bar{1}$  and *C*2/*c* phases have so far only been achieved for X = BH<sub>4</sub>.<sup>16,17</sup> Table 7 incorporates comparative bond distance and angle data for monomeric [Au(PPh<sub>3</sub>)X],<sup>19,21</sup> [M(PPh<sub>3</sub>)<sub>2</sub>X],<sup>3,8</sup> and [M(PPh<sub>3</sub>)<sub>3</sub>X]<sup>20,22,23</sup> compounds. The Cu-P bond lengths in the 2:1 molecules (*av.* 2.27<sub>0</sub> Å) are considerably shorter than those found for the 3:1 molecules (*av.* 2.35<sub>3</sub> Å) and also the 4:1 perchlorate [Cu(PPh<sub>3</sub>)<sub>4</sub>]ClO<sub>4</sub> (*av.* 2.5<sub>6</sub> Å).<sup>17</sup> Similarly the Au-P bond lengths increase from 2.24<sub>7</sub> Å for the 1:1 gold complexes to 2.32<sub>8</sub> and 2.41 Å for the 2:1 and 3:1 (X = Cl only) complexes respectively. The decrease in bond length with decreasing co-ordination number may be a reflection of decreasing steric strain, increasing strength of the M-P σ bond, and/or an increase in M-P bond order. However, the ease of ligand conformational change about the M-P bond in these complexes suggests that there is only a very small π-bonding component in the Cu-P bond. The increase in P-M-P angle of *ca.* 7° in the gold molecules can readily be interpreted in terms of the tendency of gold(I) compounds to assume a linear two-co-ordinate environment and together with the considerably longer Au-X bond by comparison with Cu-X suggests that, as expected, the Au-X bond is considerably more ionic than the Cu-X bond. Au-P distances in the 2:1 molecules are consistently *ca.* 0.05 Å longer than the analogous Cu-P distances. Both distances are however, considerably shorter than the Ag-P distances recorded for molecules containing the [Ag(PPh<sub>3</sub>)<sub>2</sub>]<sup>+</sup> unit (2.440–2.519 Å)<sup>24</sup> although here no three-co-ordinate molecule analogous to the present series has been described.

**Effect of Halide on the Core Geometry.**—Within each halide series the M-P distances and P-M-P angles are remarkably constant, the greatest difference in the P-M-P angles in either series being observed between the solvated and unsolvated forms of [Au(PPh<sub>3</sub>)<sub>2</sub>Cl] [132.1(1) *vs.* 135.7(1)°]. This halide independence of the [P<sub>2</sub>M]<sup>+</sup> core geometry is at first sight surprising, since differences in the ionic *versus* covalent character of the metal-halogen bond might be expected to be reflected in the metal-phosphorus bond parameters. The present results suggest that these parameters are relatively independent of halogen within each series. This conclusion, in fact, agrees with results obtained in SCF MS X<sub>α</sub> calculations of the bonding in [MX<sub>2</sub>]<sup>-</sup> (M = Cu or Au).<sup>25</sup> These calculations showed that the degree of covalent bonding within a given [MX<sub>2</sub>]<sup>-</sup> series is largely independent of X. The reason for this appears to be that the metal *p* orbitals involved in the bonding undergo a contraction from X = I to X = Cl, so that more favourable orbital overlap for bonding occurs for the Cl compounds. This effect compensates almost completely for the

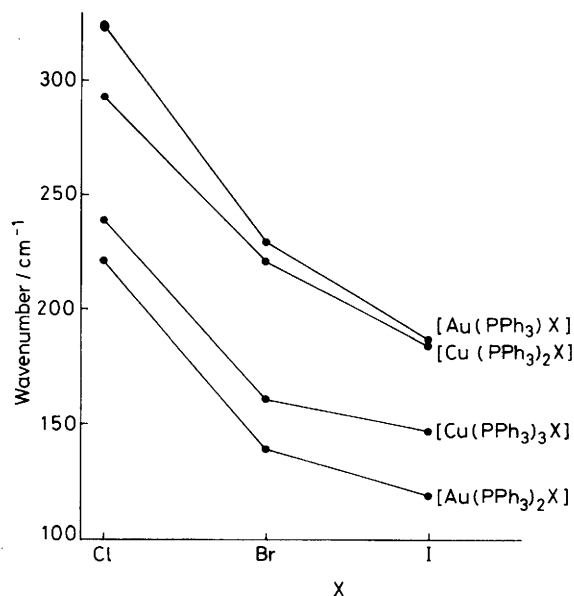
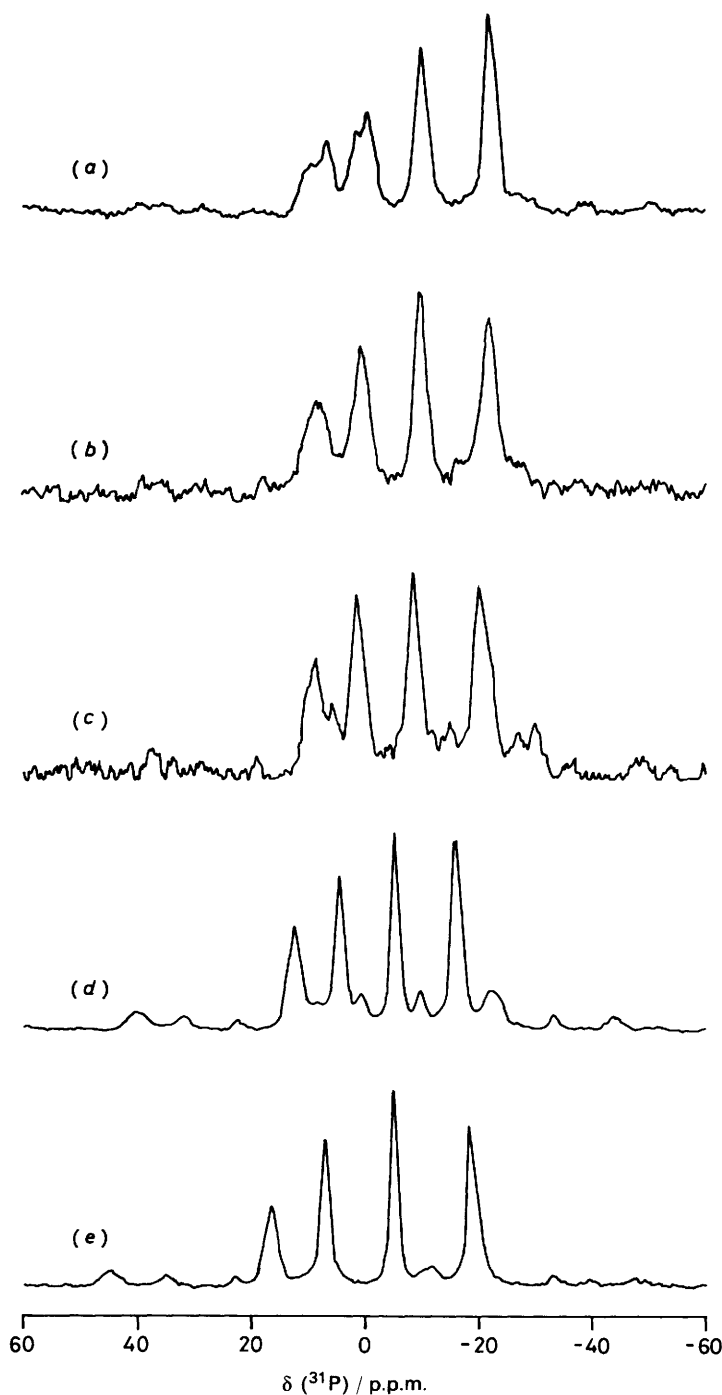


Figure 2. I.r. frequencies for the metal-halide stretch as a function of halide (X = Cl, Br, or I) and metal (M = Cu or Au)

expected greater σ donor capacity of I relative to Cl, so that the metal-halogen covalency is almost independent of halogen. Recent <sup>127</sup>I Mössbauer spectroscopic results on CuI compounds<sup>26</sup> and nuclear quadrupole resonance results for [Cu(PPh<sub>3</sub>)<sub>2</sub>Br]<sup>27</sup> have both led to suggestions that there exists a high degree of ionic character for the CuX bonds in these compounds. However, these estimates are based on the use of the Townes and Dailey method<sup>28</sup> for the analysis of the quadrupole coupling data with the assumption of *p*<sub>σ</sub> covalent bonding only, and the SCF MS X<sub>α</sub> results referred to above indicate that this approach produces estimates of the ionic character which are consistently too high. The X<sub>α</sub> results show that the CuBr bond in [CuBr<sub>2</sub>]<sup>-</sup> is approximately 50% σ covalent and about 10% π covalent. This results in a <sup>79</sup>Br coupling constant of 152.8 MHz.<sup>25</sup> For comparison, the <sup>79</sup>Br coupling constant in [Cu(PPh<sub>3</sub>)<sub>2</sub>Br] is 126.8 MHz.<sup>27</sup> This indicates a slightly more ionic CuBr bond, as expected for an increase in co-ordination number from two to three. Discussion of the relationship between the bond distance and the nature of the M-X bond is further complicated by uncertainty as to the precise role played by the triphenylphosphine ligands themselves in determining the M-X bond length and the charge distribution around the halogen. As seen from earlier discussion, the intramolecular anion-dipole interactions between the halogen and the phenyl hydrogens are likely to be both significant and influential. For comparison, analogous data for the 2:1 nitrogen-base series, [Cu(2,6Me<sub>2</sub>-py)<sub>2</sub>X]<sup>2</sup> (2,6Me<sub>2</sub>-py = 2,6-dimethylpyridine), show that in these compounds, Cu-N distances are also relatively independent of halogen [range 1.984(4)–2.004(9) Å], but that the N-Cu-N angles vary over a considerable range: 139.7(3)° for X = Cl, 142.9(2)° for X = Br, and 149.6(2) and 143.5(1)° for the α and β forms of X = I.

**Infrared Results.**—A comparison of M-X bond lengths for [Cu(PPh<sub>3</sub>)<sub>2</sub>X] and [Au(PPh<sub>3</sub>)<sub>2</sub>X] shows considerable differences, with δ = *d*(Au-X) - *d*(Cu-X) values of 0.29, 0.28, and 0.23 Å for X = Cl, Br, and I respectively. The differences for [Au(PPh<sub>3</sub>)<sub>*n*</sub>X] and [Cu(PPh<sub>3</sub>)<sub>*n*+1</sub>X] are however much less. For *n* = 1, δ = 0.07, 0.06, and 0.03 Å and for *n* = 2, δ = 0.16, 0.15, and 0.08 Å (Table 7). These effects of co-ordination



**Figure 3.**  $^{31}\text{P}$  Solid-state n.m.r. spectra of (a)  $[\text{Cu}(\text{PPh}_3)_2\text{Cl}]$ , (b)  $[\text{Cu}(\text{PPh}_3)_2\text{Br}]$ , (c)  $[\text{Cu}(\text{PPh}_3)_2\text{I}]$ , (d)  $[\text{Cu}(\text{PPh}_3)_2(\text{BH}_4)]$ , (e)  $[\text{Cu}(\text{PPh}_3)_2(\text{NO}_3)]$

number and metal atom on the M–X bond strength are reflected also in the M–X vibrational frequencies.<sup>29</sup> In the present work we have recorded the far-i.r. spectrum of  $[\text{Cu}(\text{PPh}_3)_2\text{I}]$ . Assignment of a strong band at  $184\text{ cm}^{-1}$  to the CuI terminal stretching mode is in accord with previous results for other  $[\text{M}(\text{PPh}_3)_n\text{X}]$  complexes (M = Cu or Au, Figure 2). There is a close similarity in vibrational frequencies for  $[\text{Cu}(\text{PPh}_3)_{n+1}\text{X}]$  and  $[\text{Au}(\text{PPh}_3)_n\text{X}]$ . The vibrational frequency of the isolated CuX is expected to be greater than that of AuX (e.g.  $420\text{ cm}^{-1}$  for CuCl<sup>30</sup> compared with  $383\text{ cm}^{-1}$  for AuCl<sup>31</sup>). Apparently the co-ordination of an additional molecule of triphenylphosphine

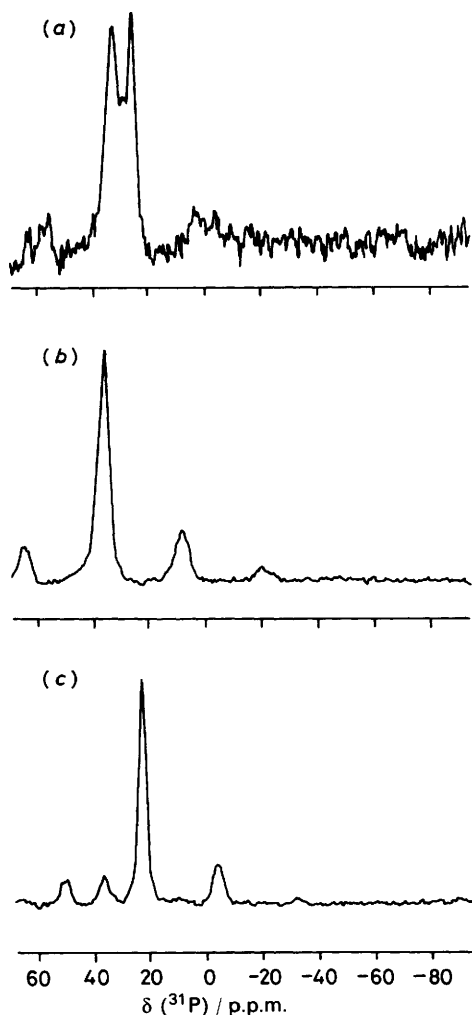
in  $[\text{Cu}(\text{PPh}_3)_{n+1}\text{X}]$  is sufficient to reduce  $\nu(\text{CuX})$  to a value similar to that of  $\nu(\text{AuX})$  in  $[\text{Au}(\text{PPh}_3)_n\text{X}]$ . However, a greater decrease in  $\nu(\text{MX})$  is observed between the two- and three-coordinate gold compounds than between the three- and four-coordinate copper compounds, reflecting again the strong preference of Au<sup>I</sup> for linear two-co-ordination.

*Solid-state  $^{31}\text{P}$  N.M.R.*—Solid-state  $^{31}\text{P}$  n.m.r. data on these compounds essentially reflects the structural characteristics described above. For the copper compounds, the signal from each crystallographically independent phosphorus is split into

**Table 8.** Solid-state cross-polarization magic-angle spinning  $^{31}\text{P}$  n.m.r. data for  $[\text{Cu}(\text{PPh}_3)_2\text{X}]^*$ 

| X             | $\delta_1$       | $\delta_2$       | $\delta_3$ | $\delta_4$ | $\langle\delta\rangle$ | $\Delta\nu_1$ | $\Delta\nu_2$ | $\Delta\nu_3$ | $\Delta\nu_{ij}$ |
|---------------|------------------|------------------|------------|------------|------------------------|---------------|---------------|---------------|------------------|
|               | p.p.m.           |                  |            |            |                        | Hz            |               |               |                  |
| Cl            | 8.1 <sup>‡</sup> | 0.3 <sup>‡</sup> | -10.2      | -22.0      | -6                     | 940           | 1 270         | 1 430         | 490              |
| Br            | 8.0              | 0.8              | -9.7       | -21.6      | -6                     | 880           | 1 280         | 1 440         | 560              |
| I             | 8.6              | 1.4              | -8.5       | -20.3      | -5                     | 880           | 1 200         | 1 430         | 550              |
| $\text{BH}_4$ | 12.6             | 4.7              | -4.8       | -15.4      | -0.8                   | 960           | 1 160         | 1 300         | 340              |
| $\text{NO}_3$ | 16.5             | 7.2              | -4.6       | -18.1      | 0.3                    | 1 120         | 1 440         | 1 640         | 520              |

\*  $\delta_i$  are chemical shift values ( $\pm 0.5$  p.p.m.) with respect to 85%  $\text{H}_3\text{PO}_4$ .  $\delta$  (solid  $\text{PPh}_3$ ) =  $-9.9$  p.p.m.;  $\langle\delta\rangle$  is the average chemical shift for each quartet;  $\Delta\nu_i$  is the spin-spin coupling interaction in Hz ( $\pm 30$ ) between each of the four peaks of the quartet;  $\Delta\nu_{ij} = \Delta\nu_i(\text{max.}) - \Delta\nu_i(\text{min.})$  is defined here as the asymmetry parameter of the quartet. <sup>‡</sup> Average values.

**Figure 4.**  $^{31}\text{P}$  Solid-state n.m.r. spectra of (a)  $[\text{Au}(\text{PPh}_3)\text{Cl}]$ , (b)  $[\text{Au}(\text{PPh}_3)_2\text{Cl}]$ , (c)  $[\text{Au}(\text{PPh}_3)_3\text{Cl}]$ 

asymmetric quartets, the magnitude of the splittings under the present experimental conditions being dependent primarily on scalar spin-spin coupling interactions with the quadrupolar copper nuclei ( $I = \frac{3}{2}$  for  $^{63}\text{Cu}$  and  $^{65}\text{Cu}$ ); with asymmetry in splitting values a consequence of quadrupolar coupling terms which are not averaged out by the magic-angle spinning technique.<sup>32,33</sup> Spectra recorded for the present series of halide complexes are reproduced in Figure 3, together with those of  $[\text{Cu}(\text{PPh}_3)_2(\text{NO}_3)]$  and  $[\text{Cu}(\text{PPh}_3)_2(\text{BH}_4)]$  for comparison. Chemical shift and splitting data are tabulated in Table 8. The

spectra for the  $C2/c$  structures ( $X = \text{I}, \text{BH}_4$ , or  $\text{NO}_3$ ) each show a single quartet as do the triclinic structures ( $X = \text{Cl}$  or  $\text{Br}$ ) although here the observed broadening and splitting of the downfield lines is consistent with the lower crystal and molecular symmetry. Only small changes in average chemical shift values occur with change of halogen:  $-6$ ,  $-6$ , and  $-5$  p.p.m. for  $X = \text{Cl}$ ,  $\text{Br}$ , and  $\text{I}$  respectively and only slightly greater shifts are observed for  $X = \text{BH}_4$  ( $-0.8$  p.p.m.) and  $X = \text{NO}_3$  ( $0.3$  p.p.m.). Overall these shifts are downfield from the 3:1 compounds,  $[\text{Cu}(\text{PPh}_3)_3\text{X}]$ :  $\text{Cl} = -10$ ,  $\text{Br} = -13$ , and  $\text{I} = -17$  p.p.m.<sup>20</sup> The asymmetry in splitting parameters of 490–560 Hz ( $\Delta\nu_{ij}$ , Table 8) reflects the lower symmetry of the charge distribution about the copper atom by comparison with the tetrahedral 3:1 compounds where  $\Delta\nu_{ij}$  fall in the range 30–60 Hz. Interestingly, the values of  $\Delta\nu_{ij}$  for the  $\text{BH}_4$  and  $\text{NO}_3$  molecules (340 and 520 Hz) are similar, despite the change in coordination number from three to four.

For the gold compounds relatively broad single lines rather than quartets are observed<sup>33,34</sup> (Figure 4). This lack of spin-spin coupling structure is likely to be a consequence of the existence of effective relaxation mechanisms because of the expected large quadrupolar moment of the gold nucleus. Phosphorus-31 chemical shift values,  $\delta$ , which are found considerably downfield from the copper analogues, are quite independent of halogen ( $\delta = 37, 38$ , and  $36$  p.p.m. for  $X = \text{Cl}$ ,  $\text{Br}$ , and  $\text{I}$  respectively). The insensitivity of  $\delta$  to minor structural change in these molecules is also reflected in identical spectra being recorded for solvated and unsolvated  $[\text{Au}(\text{PPh}_3)_2\text{Cl}]$ , despite the observed changes in  $\text{P-Au-P}$  angle for these two compounds. The  $\delta$  values are also downfield by comparison with  $[\text{Au}(\text{PPh}_3)\text{X}]$  although the spectra of the 1:1 compounds is complicated by being split into two bands; the  $\delta_{\text{av.}}$  for  $X = \text{Cl}$ ,  $\text{Br}$ , and  $\text{I}$  being 30, 32, and 36 p.p.m. respectively.<sup>19</sup> Solution values recorded for the 1:1 compounds were found to be of the order of 2 p.p.m. higher than in the solid state ( $\delta = 32, 34$ , and 38 p.p.m. for  $X = \text{Cl}$ ,  $\text{Br}$ , or  $\text{I}$ ) and 2–6 p.p.m. higher for the 2:1 compounds ( $\delta = 39, 42$ , and 42 p.p.m. for  $X = \text{Cl}$ ,  $\text{Br}$ , or  $\text{I}$ ) [ $\delta(\text{PPh}_3, \text{solution}) = -6.0$  p.p.m.]. For  $[\text{Au}(\text{PPh}_3)_3\text{Cl}]$ , the solid-state chemical shift was 23 p.p.m. which is considerably upfield from that for the two- and three-co-ordinate molecules, but downfield from the solution value of 15 p.p.m.<sup>22</sup> It seems reasonable to assume that these results also reflect the weaker  $\text{Au-P}$  bond in this molecule and the lability of the  $\text{PPh}_3$  ligand in solution. Solution values recorded for the copper compounds, while within the range found for the solid-state results showed only single relatively sharp lines which were sensitive to the concentration of triphenylphosphine and solvent, indicative of the complex equilibrium processes involved in the solution chemistry of these compounds.

## Conclusions

In summary, the results of this study show that despite the differences in the chemistries of copper(I) and gold(I), in that



gold(I) complexes tend to exist as linear, two-co-ordinate molecules while copper(I) species with soft ligands such as triphenylphosphine have a greater tendency to be four-co-ordinate, both CuX and AuX diatoms can be incorporated into  $[M(PPh_3)_2X]$  molecules with very similar molecular structures overall. While a significant fraction of the M–X bonding interactions may well be ionic rather than covalent, it is unlikely, as has been suggested,<sup>26</sup> that the attraction of  $Cu^+$  and  $X^-$  is primarily electrostatic and that there is very little or no covalent character in the bond. The present array of results tend to support the presence of covalent interactions, but their influence on the spectroscopic and structural parameters may well be minimized by the types of mechanisms suggested as a result of the SCF MS  $X\alpha$  calculations.

It is clear, chemically, that the packing requirements of the triphenylphosphine ligands are a major factor in determining the unusual stability of the copper compounds with respect to addition or dimerization reactions. In addition, intramolecular anion–dipole interactions between the halogen and the phenyl hydrogens, which are made possible through the conformational flexibility of triphenylphosphine about the M–P and P–C bonds, may assist in stabilizing the gold compounds against dissociation of the halogen to form purely ionic  $[M(PPh_3)_2]X$ .

### Acknowledgements

We gratefully acknowledge support of this work by a grant from the Australian Research Grants Scheme. The Bruker CXP-300 spectrometer is operated by the Brisbane N.M.R. Centre and we thank the Centre for making instrumental time available to us. Carbon and H analyses were completed by the University of Queensland microanalytical service.

### References

- J. C. Dyason, L. M. Engelhardt, P. C. Healy, C. Pakawatchai, and A. H. White, *Inorg. Chem.*, 1985, **24**, 1951.
- J. C. Dyason, P. C. Healy, C. Pakawatchai, V. A. Patrick, and A. H. White, *Inorg. Chem.*, 1985, **24**, 1957.
- P. H. Davis, R. L. Belford, and I. C. Paul, *Inorg. Chem.*, 1973, **12**, 213.
- P. G. Eller, G. J. Kubas, and R. R. Ryan, *Inorg. Chem.*, 1977, **16**, 2454.
- J. C. Dyason, L. M. Engelhardt, C. Pakawatchai, P. C. Healy, and A. H. White, *Aust. J. Chem.*, 1985, **38**, 1243.
- A. Cassel, *Acta Crystallogr., Sect. B*, 1979, **35**, 174.
- B.-K. Teo and J. C. Calabrese, *J. Chem. Soc., Chem. Commun.*, 1976, 185.
- N. C. Baenziger, K. M. Dittmore, and J. R. Doyle, *Inorg. Chem.*, 1974, **13**, 805.
- M. Khan, C. Oldham, and D. G. Tuck, *Can. J. Chem.*, 1981, **59**, 2714.
- F. A. Cotton and D. M. L. Goodgame, *J. Chem. Soc.*, 1960, 5267.
- F. Cariati and L. Naldini, *J. Inorg. Nucl. Chem.*, 1966, **28**, 2243.
- J. M. Meyer and A. L. Allred, *J. Inorg. Nucl. Chem.*, 1968, **30**, 1328.
- P. F. Barron, J. C. Dyason, L. M. Engelhardt, P. C. Healy, and A. H. White, *Aust. J. Chem.*, 1985, **38**, 261.
- 'International Tables for X-Ray Crystallography,' eds. J. A. Ibers and W. C. Hamilton, Kynoch Press, Birmingham, 1974, vol. 4.
- S. R. Hall, The XTAL User Manual, Technical Report of the Computer Science Centre, University of Maryland, U.S.A., 1983.
- S. J. Lippard and K. M. Melmed, *Inorg. Chem.*, 1967, **6**, 2223.
- L. M. Engelhardt, C. Pakawatchai, A. H. White, and P. C. Healy, *J. Chem. Soc., Dalton Trans.*, 1985, 125.
- G. G. Messmer and G. J. Palenik, *Inorg. Chem.*, 1969, **8**, 2751.
- P. F. Barron, P. C. Healy, J. Oddy, L. M. Engelhardt, and A. H. White, *Aust. J. Chem.*, in the press.
- P. F. Barron, J. C. Dyason, P. C. Healy, L. M. Engelhardt, C. Pakawatchai, V. A. Patrick, and A. H. White, following paper.
- N. C. Baenziger, W. E. Bennett, and D. M. Soboroff, *Acta Crystallogr., Sect. B*, 1976, **32**, 962.
- P. G. Jones, G. M. Sheldrick, J. A. Muir, M. M. Muir, and L. B. Pulgar, *J. Chem. Soc., Dalton Trans.*, 1982, 2123.
- J. T. Gill, J. J. Mayerle, P. S. Welcker, D. F. Lewis, D. A. Ucko, D. J. Barton, D. Stowens, and S. J. Lippard, *Inorg. Chem.*, 1976, **15**, 1155.
- P. F. Barron, J. C. Dyason, P. C. Healy, L. M. Engelhardt, B. W. Skelton, and A. H. White, *J. Chem. Soc., Dalton Trans.*, 1986, 1965.
- G. A. Bowmaker, P. W. D. Boyd, and R. J. Sorrenson, *J. Chem. Soc., Faraday Trans. 2*, 1985, 1627.
- R. J. Batchelor and T. Birchall, *J. Chem. Soc., Dalton Trans.*, 1985, 1727.
- H. Negita, M. Hiura, Y. Kushi, M. Kuramoto, and T. Okuda, *Bull. Chem. Soc. Jpn.*, 1981, **54**, 1247.
- E. A. C. Lucken, 'Nuclear Quadrupolar Coupling Constants,' Academic Press, London, 1969, p. 120.
- G. A. Bowmaker and D. A. Rogers, *J. Chem. Soc., Dalton Trans.*, 1984, 1249.
- T. P. Martin and H. Schaber, *J. Chem. Phys.*, 1980, **73**, 3541.
- K. P. Huber and G. Herzberg, 'Constants of Diatomic Molecules,' D. Van Nostrand, New York, 1979.
- E. M. Menger and W. S. Veeman, *J. Magn. Reson.*, 1982, **46**, 257.
- J. W. Diesveld, E. M. Menger, H. T. Edzes, and W. S. Veeman, *J. Am. Chem. Soc.*, 1980, **102**, 7935.
- N. J. Clayden, C. M. Dobson, K. P. Hall, D. M. P. Mingos, and D. J. Smith, *J. Chem. Soc., Dalton Trans.*, 1985, 1811.

Received 10th June 1986; Paper 6/1173